Tropical Intraseasonal Modes of the Atmosphere

Yolande L. Serra,[1] Xianan Jiang,[2,3] Baijun Tian,[3] Jorge Amador-Astua,[4] Eric D. Maloney,[5] and George N. Kiladis[6]

[1]Department of Atmospheric Sciences, University of Arizona, Tucson, Arizona 85721-0081; email: serra@email.arizona.edu

[2]Joint Institute for Regional Earth System Science & Engineering, University of California, Los Angeles, California 90095; email: xianan@jifresse.ucla.edu

[3]Jet Propulsion Laboratory, California Institute of Technology, Pasadena, California 91109; email: baijun.tian@jpl.nasa.gov

[4]School of Physics and Center for Geophysical Research, University of Costa Rica, San Jose, Costa Rica, 11501-2060; email: jorge.amador@ucr.ac.cr

[5]Department of Atmospheric Science, Colorado State University, Fort Collins, Colorado 80523-1371; email: emaloney@atmos.colostate.edu

[6]Physical Sciences Division, Earth System Research Laboratory, National Oceanic and Atmospheric Administration, Boulder, Colorado 80305-3328; email: george.n.kiladis@noaa.gov

Annu. Rev. Environ. Resour. 2014. 39:189–215

First published online as a Review in Advance on August 13, 2014

The *Annual Review of Environment and Resources* is online at environ.annualreviews.org

This article's doi:
10.1146/annurev-environ-020413-134219

Keywords

multiscale variability, Madden-Julian oscillation, convectively coupled equatorial waves, tropical convection, convective organization, atmospheric transport

Abstract

Tropical intraseasonal variability (TISV) of the atmosphere describes the coherent variability in basic state variables, including pressure, wind, temperature, and humidity, as well as in the physical phenomena associated with the covariability of these parameters, such as rainfall and cloudiness, over synoptic (~1,000 km, ~1–10 days) to planetary (~10,000 km, ~10–100 days) scales. In the past, the characteristics of individual TISV modes were studied separately, and much has been learned from this approach. More recent studies have increasingly focused on the multiscale nature of these modes, leading to exciting new developments in our understanding of tropical meteorology. This article reviews the most recent observations of TISV and its associated impacts on regional weather, short-term climate patterns, and atmospheric chemical transports, as well as the ability of numerical models to capture these interacting modes of variability. We also suggest where the field might focus its efforts in the future.

Contents

1. INTRODUCTION

Tropical intraseasonal variability (TISV) of the atmosphere describes the coherent variability in basic state variables, including pressure, wind, temperature, and humidity, as well as in the physical phenomena associated with the covariability of these parameters, such as rainfall and cloudiness, over synoptic (~1,000 km, ~1–10 days) to planetary (~10,000 km, ~10–100 days) scales. The global tropical atmosphere exhibits distinct modes of TISV that dominate the observed variability in the location and timescales of tropical deep convection (**Figure 1**) (1, 2) and that are important physical mechanisms by which momentum, heat, and moisture are transported between the tropics and extratropics (2–4). The potential to exploit these distinct modes of TISV to enhance the accuracy of extended-range forecasts of the tropics and extratropics is hampered by the current state of understanding of the nonlinear, multiscale nature of these modes and their poor simulation in global models (1, 5, 6).

Equatorial Rossby (ER) waves: a westward mode with eastward or westward energy propagation

Inertio-gravity (IG) waves: an eastward (EIG) or westward (WIG) mode with eastward or westward energy propagation

Mixed-Rossby gravity (MRG) waves: a westward mode with eastward energy propagation

Kelvin waves: an equatorial wave with zonal wind oscillations at maximum on the equator and with eastward phase and energy propagation

Since the early studies of easterly waves by Riehl (7), we have known that a substantial portion of TISV is organized by large-scale waves that propagate parallel to the equator. Assuming restoring forces of rotation and gravity, and neglecting moist processes, Matsuno (8) used the linearized shallow-water equations of motion on an equatorial beta plane to show that there are several distinct zonally propagating classes of solutions to the motion that are trapped within a characteristic length scale from the equator. Matsuno showed that the structure of the kinematic fields of these waves, including their divergent flow, was either symmetric (like signed) or antisymmetric about the equator.

Two such classes of solutions correspond to equatorial Rossby (ER) and inertio-gravity (IG) waves. ER waves result in symmetric perturbations of flow and divergence in the form of alternating cyclonic and anticyclonic gyres centered on lines of constant latitude, and these waves are more rotational in character. In other solutions, including mixed-Rossby gravity (MRG) waves, longer wavelengths behave like Rossby waves, and shorter wavelengths behave like gravity waves. Equatorial Kelvin waves are also a solution to Matsuno's equations. The structure and

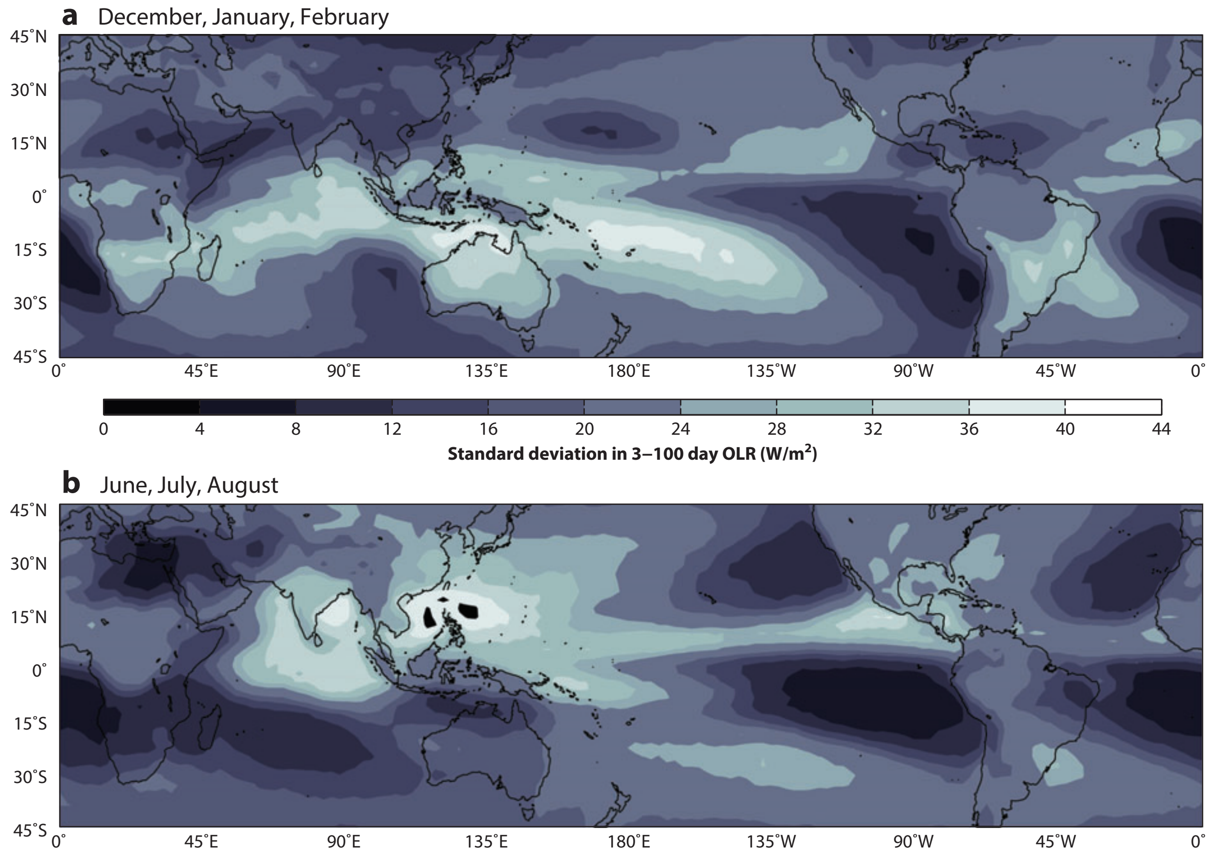

Figure 1

The standard deviation in 3–100-day filtered outgoing long-wave radiation (OLR) (22 W/m^2 contour only) for (*a*) December, January, February and (*b*) June, July, August. OLR climatology is based on 1979–2010.

characteristics of these solutions have been described in detail in several previous studies (1, 9–11). Similar equatorially trapped modes are also observed in the ocean but are not discussed in this review.

Initial interest in Matsuno's waves stemmed from their potential ability to explain oscillations observed in the stratosphere, known as the quasi-biennial oscillation (12). With the advent of satellites that observe Earth's clouds from space, scientists realized that these discrete modes not only existed as dry waves in the stratosphere but also were coupled to convection in the tropical troposphere (9, 11, 13–15). The structure of a convectively coupled equatorial wave (CCEW) is significantly different from its dry wave counterparts, and convection acts to slow the phase speeds of the disturbances (1, 9, 11).

Cross-spectral methods of identifying these modes in observations also led to the discovery of an additional mode, not described by Matsuno's equations, referred to as the Madden-Julian oscillation (MJO) after the authors who first identified it in island station zonal wind and pressure observations (16, 17). The disturbance has characteristics of forced Kelvin and ER waves (18, 19) associated with a convective envelope that travels eastward at about 5 m/s with a period of

Convectively coupled equatorial wave (CCEW): an atmospheric wave coupled to convection in the tropical troposphere through the wave's divergence aloft

Madden-Julian oscillation (MJO): a convective center with equatorial zonal wind anomalies to the east and off-equatorial Rossby gyres to the west

30–90 days. The MJO is present year round, but it is strongest in the Eastern Hemisphere during the boreal winter. It has been associated with important atmospheric phenomena across many time and space scales, including the modulation of global tropical cyclone (TC) activity (20–24) and global monsoon convection (25–28), as well as the onset/termination of El Niño events (29–31). As is discussed below, current research is focused on understanding the physical mechanisms responsible for forcing and maintaining this disturbance, its regional manifestations throughout the global tropics, and the complex multiscale interactions associated with it.

Tropical depression (TD)-type waves: synoptic-scale off-equatorial westward-moving gyres with periods of four to six days

Intertropical convergence zone (ITCZ): a confluence of the Northern and Southern Hemisphere trade winds characterized by deep convection

Although also not an equatorially trapped solution to Matsuno's equations, easterly waves or tropical depression (TD)-type waves (7) are part of the continuum of Rossby wave-like disturbances in the tropics (32–40). Despite evidence that TD-type waves travel from the Atlantic into the Pacific (41, 42), several in situ forcing mechanisms within the eastern Pacific have also been proposed (43–49). TD-type structures can also evolve from or into MRG waves in response to the background flow (38, 39, 50, 51). These disturbances were linked as early as the 1940s to TC genesis in the Atlantic (7) and, more recently, to TC genesis in the eastern (44, 51–55) and western (55–60) Pacific basins. By contrast, they may also form from energy dispersed from TCs in the western Pacific (51).

This review assesses our current understanding of CCEWs, the MJO, and TD-type waves not as independent disturbances but as a collective organizing mechanism for convection in the tropics. We restrict this discussion to intraseasonal and higher-frequency multiscale interactions within the intertropical convergence zone (ITCZ) and monsoon regions of the Northern Hemisphere, although such interactions exist throughout the global tropics [including the Australian (61) and South American (62) monsoons] and are the primary link between regional weather and the large-scale circulation of the atmosphere. The concept of multiscale variability has gained recent attention in the literature on tropical meteorology (63, 64), with implications for the extratropics (65). Thus, although we have begun this review by introducing the distinct modes of TISV—which has been a productive way of characterizing the individual modes over the past few decades—this approach to understanding tropical convection is undergoing a transition. New theoretical constructs are emerging to better model the multiscale nature of tropical rainfall in observations, and these new constructs allow us to better represent TISV modes in numerical models and to exploit their inherent predictability to improve extended forecasts of the tropics and extratropics.

This article is organized as follows: We first review the most recent observational evidence for the multiscale nature of TISV and its impact on regional weather, short-term climate patterns, and atmospheric chemical transports; we then review the current ability of numerical models to capture these interacting modes of variability. Finally, we suggest where the field might focus its efforts in the future.

2. PHENOMENOLOGY OF TROPICAL INTRASEASONAL VARIABILITY

Over the past few decades, satellite remote sensing technology has expanded from simply providing global visible and infrared imagery to providing global estimates of precipitation, total column water vapor fields, vertical moisture and temperature profiles, and cloud optical properties and depths (66–70). These satellite observations, together with improved in situ measurement capabilities (71, 72) and global reanalysis data sets (73), have led to the continued advancement in our understanding of TISV modes and their interactions since their discovery several decades ago.

A few recent publications have reviewed the current state of research on TISV, focusing on CCEWs (1) and the MJO (19, 64). Here, we review empirical studies of TISV specifically related to the multiscale nature of the MJO and CCEWs. The interested reader is referred to these more detailed reviews for the mathematical derivations of the modes and their individual characteristics.

2.1. Indo-Pacific

2.1.1. Madden-Julian oscillation. Visual inspection and spectral analysis of the MJO convective envelope in the Indo-Pacific region using outgoing long-wave radiation (OLR) from satellites suggest that the MJO in this region consists of smaller-scale cloud elements organized on meso (∼100–500 km) to planetary scales that propagate both eastward and westward within the overall eastward-propagating MJO envelope (2, 59, 74–76). An early schematic of this multiscale interaction based on satellite infrared images (74) indicates westward-moving mesoscale convective systems (MCSs) (77) within eastward-moving super cloud clusters. The westward-moving MCSs are associated with CCEWs, including westward IG (WIG) waves, MRG waves, and TD-type disturbances. Some studies additionally suggest that the eastward-propagating MJO includes stationary wave components (78, 79). Investigators find that TC activity clusters during the convectively active phase of the MJO over the warm pool region of high sea surface temperature (SST) in all tropical ocean basins (80–86).

Atmospheric river: a stream of moist air transported from the tropics to the midlatitudes by midlatitude cyclones

Boreal summer intraseasonal oscillation (BSISO): the northward component of the Indo-Pacific intraseasonal oscillation specific to the warm season

In regions of low-level westerly winds in the convective envelope of the MJO, OLR variance in the Kelvin to MJO wave number–frequency band forms a space-time continuum (76, 87, 88). In contrast, OLR variance in these two bands remains separate in regions of easterly flow when convective coupling is weak and Kelvin wave speeds increase. This suggests that, during the convectively suppressed phase of the MJO, Kelvin wave activity is modified by the lower-frequency basic state (87, 88). Consistent with this finding, convection associated with Kelvin waves is found to be enhanced within the MJO convective envelope as it forms over the Indian Ocean, but this activity moves to the east of the MJO envelope as the MJO reaches the western Pacific (59). Kelvin wave activity in the central Pacific is additionally hypothesized to result from more favorable conditions for extratropical Rossby wave energy propagation into the tropics over Australia during the active phase of the MJO in the western Pacific, which appears linked at times to the forcing of Pacific Kelvin waves (59).

Although the Indo-Pacific MJO convective envelope contains CCEWs, its initiation shows few effects caused by specific CCEW disturbances (89, 90). Primary MJO events, defined as those events without a preceding MJO cycle, appear to initiate in situ with no evidence of midlatitude lateral forcing; globally propagating equatorially trapped circulations; or local anomalies in boundary-layer convergence, tropospheric humidity, or SSTs (89, 91). Observed evidence of these initiation mechanisms appears to be limited to successive MJO events in which a previous MJO cycle can be identified (91, 92). Primary MJO deep convective events are found to be preceded by global-scale circulation anomalies and suppressed convection over the western Pacific (89), as well as over the Indian Ocean in some studies (91).

Indo-Pacific MJO events are far-reaching with trans-Pacific Rossby wave trains emanating from their large convective centers and appearing similar to those observed in association with tropical interannual modes (93). In the central and eastern Pacific during boreal winters, these wave trains modulate atmospheric river events, which bring heavy rainfall to the western United States (94). Indo-Pacific wave trains also modulate North American monsoon (NAM) precipitation during the boreal summer, with the largest influence observed over Mexico (21). During the boreal winter and spring, MJO signals are observed propagating eastward from the Indo-Pacific to the Atlantic across Panama and the Caribbean Sea, influencing the tropical and subtropical Atlantic (95). MJO–El Niño–Southern Oscillation (ENSO) interactions, which are beyond the scope of this review, also play potentially important roles in global weather patterns (96).

2.1.2. Northward-propagating mode. Although the boreal winter MJO in the Indo-Pacific primarily propagates eastward, the boreal summer intraseasonal oscillation (BSISO), a version of the

MJO, has a dominant northward component resulting from complex, and as yet not fully understood, feedback processes with the background monsoonal circulation. The BSISO is associated with active and break periods of the Asian monsoon (97), and thus its predictability has significant socioeconomic importance to this region of the world (98). TCs are also four times more likely to be associated with BSISO activity than the MJO during the boreal summer (23), adding to their significance for the region.

A leading hypothesis for the northward propagation of this mode is an instability that arises within the background mean state during the monsoon. First, a zonally symmetric cloud band embedded in a mean easterly zonal shear, like that observed during the Asian monsoon, produces a barotropic cyclonic vorticity anomaly north of the convection. The resulting frictionally driven boundary-layer moisture convergence then favors new convection within the vorticity anomaly to the north (99). Second, perturbation moisture resulting from advection by both mean and perturbation meridional flows shows a maximum north of the convective center (99, 100), again favoring convection to the north of the convective center. The former process dominates away from the equator, and the latter process dominates near the equator. This mechanism is not linked to the eastward-propagating mode and thus can explain independent northward-propagating events observed in the region (99), which occur for a significant fraction of the cases (101). It should also be noted that Kelvin wave activity appears to be decoupled from the northward-propagating mode, whereas MRG waves, ER waves, and TD-type disturbances remain coupled to the BSISO envelope as it propagates northward (59). Air-sea interactions, with higher intraseasonal SST anomalies to the north of the convective center, also likely play a role in northward propagation in addition to the other proposed mechanisms (102, 103).

2.1.3. The 10–30-day mode. In addition to the eastward- and northward-propagating modes on 30–90-day timescales, 10–30-day oscillations are also observed during the boreal summer in the Indo-Pacific region, where they significantly modulate Indian and Asian monsoon rainfall patterns (104–108) and western Pacific TC activity (109). This mode consists of a pair of counter-circulating Rossby gyres that initiate over the western Pacific and propagate westward along the equator and 15°–20°N, with the northern track corresponding to the southern edge of the Indian monsoon trough (104, 110). Rossby waves are also observed emanating from convection over the equatorial Indian Ocean (110). Rossby gyres frequently form symmetrically about the equator; as the monsoon season progresses, the background easterly shear, warm SSTs, and enhanced moisture availability north of the equator favor growth of the northern gyres (103, 110). Boundary-layer frictional convergence of moisture within the cyclonic Rossby gyres to the north may also contribute to the northward propagation of the BSISO associated with instabilities in the background flow described in the previous section (103, 110, 111), although the relative importance of each process linking these scales of variability is unclear (103). Some evidence also exists for initiation of the 10–30-day mode by extratropical Rossby waves entering the tropics over East Asia (105, 107). Like the Indo-Pacific MJO, the 10–30-day mode over the western north Pacific is also associated with the NAM through a notable trans-Pacific Rossby wave train (80). NAM variability is dominated by this 10–30-day mode, with the MJO having a secondary role (21).

Although these studies suggest that the 10–30-day westward-propagating mode may contribute to the coupling of the 30–90-day eastward- and northward-propagating modes, evidence also exists for the independence of these low-frequency modes. In particular, weak Indian monsoon (i.e., BSISO) years correspond to strong eastward-propagating MJO activity with amplitudes comparable to those in the winter (112). Off-equatorial divergence generates a Rossby gyre that propagates northwestward over India, reinforcing the suppressed phase of the BSISO. Conversely, strong Indian monsoon years with heavy flooding correspond to weak eastward-propagating MJO activity (112). Strong evidence also exists for an association between the MJO, Kelvin waves, and monsoon onset over India (113) and the South China Sea (114). A unified theory describing the multiscale variability of the TISV associated with the Asian monsoon must account for both the independence and covariability of these modes. It must also account for the interactions of these modes with the higher-frequency variability described next.

2.1.4. Higher-frequency variability. Westward-propagating CCEWs are favored through the wave accumulation mechanism (115) in areas of zonal wind convergence, as observed in the western Pacific where the monsoon westerlies meet the trade winds (51, 116). These conditions are enhanced (suppressed) during the active (suppressed) phase of the MJO over the western Pacific (51, 58). TC growth is also favored in regions of low-level zonal convergence (57), and these disturbances can then be a source of TD-type disturbances in the region (51). Transitions from MRG waves to TD-type disturbances are also favored in the western Pacific confluence zone, where the longer waves become shorter and intensify (51).

Energetics analysis of the submonthly flow in the western Pacific during the boreal summer indicates that barotropic energy conversions are enhanced during the active phase of the MJO (22). The dominant contributions to these conversions are associated with the convergence and shear of the zonal mean wind, suggesting that wave accumulation and barotropic conversions are important to eddy growth in the region. However, it remains unclear if these dynamic growth mechanisms are sufficient for TC genesis. Studies suggest that most TCs in the western Pacific form in association with the monsoon convergence zone, where MCSs appear to play an important role in their formation (57, 60). It may be that the MJO creates conditions favorable for the growth of eddies to some finite amplitude where further growth is possible because of convective processes (51, 58). Other studies have shown that vortices associated with mesoscale convection can form and grow within a larger TD trough when the smaller-scale structures and the wave trough travel at similar speeds, creating a so-called critical layer (60). In this slowly moving frame, the TD trough provides a favorable and isolated environment for intensification of one or more mesoscale systems that organize, strengthen, break away from the larger TD trough, and eventually develop into a TC. Although this theory allows for the importance of upscale intensification through aggregation of smaller vortices, initial vortex formation and growth rely on support from the synoptic to meso scale.

2.2. Eastern Pacific

The tropical eastern Pacific in the Northern Hemisphere is connected to the relatively smaller NAM system compared to that of the Asian monsoon and is additionally bordered to the south by cold SSTs along the equator and land to the east, separating it from the Atlantic. These factors greatly impact the TISV in the basin (117), which differs significantly from that of the Indo-Pacific. In particular, MJO convective coupling is significantly weaker in this basin than in the Indo-Pacific, land-falling TCs are less frequent owing to the predominantly easterly flow, and Atlantic variability has a significant impact on the eastern Pacific over a range of timescales from intraseasonal to interannual. The TISV of this basin has received notably less attention in the literature than that of the Indo-Pacific, although recent studies have uncovered modes of TISV in the region that, like their Indo-Pacific counterparts, have potentially important socioeconomic impacts on the populations of both North and Central America.

2.2.1. The 30–90-day mode. Unlike the Indo-Pacific, intraseasonal variability on 30–90-day timescales in the tropical eastern Pacific (118) has a maximum amplitude during the boreal summer (40). The 30–90-day mode has a spatial structure similar to that of the Indo-Pacific MJO and will hereafter be referred to as the eastern Pacific MJO. The origins of the eastern Pacific MJO are unclear. Early studies used global MJO indices to study the nature of the disturbance in the eastern Pacific, thus demonstrating that it is at least in part phase locked to the Indo-Pacific mode (20, 22, 75), but more recent studies have isolated the mode in eastern Pacific rainfall observations (118, 119). Modeling studies suggest the possibility that the eastern Pacific MJO can exist independently of the Indo-Pacific MJO but also that the two can phase lock (120). The warmer SSTs north of the equator in this basin shift the surface convergence maximum off the equator (121, 122), likely contributing to the off-equatorial convective maximum here (75, 121).

The eastern Pacific MJO, like its Indo-Pacific counterpart, exhibits northward as well as eastward propagation (119, 123). A distinct north-south structure in the moisture and wind fields is evident in association with this mode (75, 122), but the upper-level winds are more consistent with the eastward-propagating mode (122). It is hypothesized that the natural barrier produced by the topography of the Americas not only acts as a terminus for the eastward progression of the low-level signal of the MJO in this basin but also provides an upstream feedback for the structure of the low-level signal (122). The mean easterly vertical shear also supports a propagation mechanism similar to that hypothesized for the BSISO associated with the Asian monsoon, whereby generation of positive vorticity and moisture anomalies to the north of convection results from an unstable mode of the mean state (119). It remains to be discovered what impact if any the land barrier downstream of the barotropically unstable flow, as described by Jiang & Waliser (119), has on the meridional propagation of the mode in this basin.

2.2.2. The 10–30-day modes. In addition to the 30–90-day mode, the eastern Pacific also exhibits variability on 10–30-day timescales (118, 124). The dominant mode in eastern Pacific rainfall propagates eastward and then northward upon entering the eastern Pacific (118). This mode is also visible in Caribbean, Gulf of Mexico, and western Atlantic rainfall anomalies (118). In a separate study, the dominant mode in the western Atlantic, Caribbean, Gulf of Mexico, and eastern Pacific OLR is found to propagate westward from Africa along 15°N and is referred to as the west-east mode. A second mode appears more similar to that of the eastern Pacific rainfall mode (118), propagating eastward from the western Pacific and then northward into North America, and is referred to as the north-south mode (124).

The west-east mode may be an extension of an ER wave mode associated with the African monsoon (124), discussed below in Section 2.4.2. The north-south mode has some signature in the NAM region but is not correlated with the 10–30-day TISV found in Arizona–New Mexico (AZNM) precipitation (21, 80) and is not associated with a trans-Pacific Rossby wave train as observed with the AZNM mode (80, 118). Further study is required to determine if the AZNM 20-day mode is a local manifestation of the north-south mode or if these are separate phenomena. It also remains to be discovered whether the north-south mode in the eastern Pacific is of local origin (118) or if it is associated with convection in the western Pacific, as implied by the west Pacific origins of the equivalent OLR mode (124).

The 10–30-day northward-propagating mode in the eastern Pacific is generally more active when the 30–90-day mode is suppressed (118). This anticorrelation between the modes does not appear to be related to interannual variability in SST such as ENSO (118). Possible scale selection by the background flow should be explored.

2.2.3. Higher-frequency variability. As in the Indo-Pacific, westward-propagating disturbances are found embedded in eastern Pacific MJO convective envelopes (122, 125, 126). Similarly, barotropic dynamics favor eddy activity during the eastern Pacific MJO active phase; however, the relative role of the zonal wind convergence versus the meridional shear of the zonal wind in supporting this activity remains unclear (22, 122, 126). It also remains to be seen whether these instabilities in the flow can support local generation of TD-type disturbances or whether preexisting finite amplitude disturbances are required. A portion of the TD-type disturbances initiated over Africa are observed to propagate into the eastern Pacific (41, 42), but it remains uncertain what the primary source of seed disturbances might be for this basin.

TCs are also enhanced during the active phase of the eastern Pacific MJO (20, 85, 122, 126–128), with some results additionally suggesting an even greater impact on the suppression of TCs during the inactive phase (122). Interaction of TD-type disturbances with the topography of Central America and Mexico is also found to favor leeside development of TCs (54, 129). Orographic forcing may be enhanced during the active phase of the MJO when TD-type waves and TC tracks are shifted northward along the west coast of Mexico and into the Gulf of Mexico (122, 126).

Intra-Americas Sea (IAS) region: the tropical-subtropical west Atlantic and far northeastern Pacific, Caribbean Sea, Gulf of Mexico, and adjacent land areas

Caribbean low-level jet (CLLJ): a tongue of maximum low-level easterly flow across the Caribbean Sea

2.3. Intra-Americas Sea Region

Seasonal, intraseasonal, and diurnal precipitation events in the Intra-Americas Sea (IAS) region are associated with TD-type disturbances (7), cold front intrusions from midlatitudes (130, 131), *temporales* (periods of weak to moderate rainfall lasting several days) (132, 133), TCs (134), and low-frequency global-scale modulators (such as ENSO). Different precipitation regimes in the eastern and western Caribbean and the Pacific slopes of Central America and southern Mexico emerge as a result of the interaction of the Caribbean low-level jet (CLLJ) with multiscale processes, including low-frequency modulators (47, 135). The role of the Atlantic and Pacific SSTs in the onset and end of the rainy season (136) and in the disruption of rainfall in July and August along the Pacific coast of Central America and southern Mexico, known as the midsummer drought (137), are just two components of a complex problem of multiscale interactions (47). The contribution of intraseasonal variability to the annual cycle in precipitation over Central America and the Caribbean is still an open research problem.

Heavy rain events throughout the Caribbean are related to 30–90-day variability in the CLLJ associated with the global MJO pattern through variability in the low-level divergence fields (138). The modulation is most significant in the months from September through November but is observed throughout the year. The MJO has also been associated with large rainfall variability along the Pacific coast, over southern Mexico and Central America, and along the Gulf coast of Mexico (64, 139).

Strong synoptic and shorter-scale variability in SST, air temperature, pressure, and specific humidity were observed during the *Experimento Climático en las Albercas de Agua Cálida* (ECAC) Phase 3 campaign for the period July 7–24, 2001, especially in the vicinity of the CLLJ core (135). Similarly, the atmospheric mixed-layer height showed considerable small- and synoptic-scale fluctuations near and below the CLLJ core during this time. A comparison of observed air temperature, specific humidity, and wind profiles, as well as sensible and latent heat fluxes and wind stress, with those of reanalyses at grid points close to the observations, indicates large deficiencies in these parameters in the gridded products (135).

Previous studies have shown that the sign of the meridional gradient of potential vorticity reverses in the western Caribbean and eastern Pacific during summer (44, 140), allowing, if proper conditions are met, the exchange of kinetic energy between the mean flow and tropical disturbances, such as TD-type waves (46, 141), similar to what is observed in the western Pacific. A strong CLLJ favors these barotropic conversions over the far eastern Pacific (46), although the exact relationship between TD-type waves and the CLLJ remains unclear (47). A strong jet is also positively correlated with increased eastern Pacific TC activity, consistent with an increase in TD-wave activity (46). The CLLJ and MJO indices used in Serra et al. (46) are uncorrelated, indicating that the modulation of TD-type waves and TCs by the jet is independent of that by the MJO.

Quasi-biweekly zonal dipole (QBZD): the primary 10–30-day mode over central and western Africa during the boreal summer

The above results stress the importance of the CLLJ as an energy source for waves and potential TC development in the IAS, but the findings also pose some scientific challenges with regard to the CLLJ structure and dynamics over this region. In particular, the vertical wind shear over the region increases as the CLLJ develops, so TC activity is at a minimum during July in the Caribbean (142). In addition, as the CLLJ crosses Central America from the Caribbean into the Pacific near Costa Rica and Nicaragua, the jet core is located at higher levels (about 1,500 m above sea level) than over the Caribbean jet core (800 m above sea level). It is unclear what physical processes maintain the CLLJ and lift the jet core as it crosses into the Pacific. The possibility of the waves providing energy to the mean flow to maintain the CLLJ during the summer needs to be further explored (141).

2.4. Africa

2.4.1. The 30–90-day modes. The ITCZ over Africa and the eastern Atlantic exhibits a stationary pulse in convective activity on 30–90-day timescales that is significantly correlated with the Indo-Pacific MJO (25, 27). This 30–90-day mode is characterized by an eastward-propagating dry (i.e., uncoupled to convection) equatorial Kelvin wave from the Atlantic meeting a westward-propagating dry ER wave, following a suppressed phase in the Indo-Pacific MJO over the western equatorial Pacific and an active Indian monsoon (25, 143). Midtropospheric negative temperature anomalies and enhanced surface westerlies associated with the Kelvin wave from the Atlantic combine with low-level easterlies associated with the ER wave from the Indian sector. These mechanisms enhance monsoon rainfall over Africa for about 20 days following suppressed (active) convection over the equatorial western Pacific (India).

Moreover, the 30–90-day stationary mode also consists of an initially dry westward-propagating ER wave along the northern edge of the African monsoon region with a 40–45-day periodicity that appears to emanate from active convection over India (143, 144). As the Rossby wave propagates over Africa, it is associated with enhanced eastward moisture transports and convection, while the convection within and south of the ITCZ simultaneously builds across west and central Africa as part of the stationary response of this mode (143). The Rossby wave forced by the MJO may first initiate convection over the Darfur highlands, which is a sensitive location for forcing TD-wave activity over west Africa (35, 84).

The 30–90-day mode can modulate the African monsoon onset, as noted by Janicot et al. (145) for the 2006 monsoon. In this case, a warm anomaly associated with a Kelvin wave that emanated from a suppressed MJO event in the equatorial western Pacific in mid-June traveled eastward and met a westward-propagating ER wave over Africa in late June, delaying the onset of the African monsoon into mid-July.

2.4.2. The 10–30-day modes. The Guinean or quasi-biweekly zonal dipole (QBZD) mode is a stationary pattern colocated with the ITCZ with opposing centers of activity along the Guinean coast and off the coast of South America near 40°W (146). A mechanism is proposed whereby low surface pressure anomalies associated with strong surface heating during a suppressed period of convection over west Africa induces eastward moisture transport from the eastern Atlantic. In some cases, arrival of an equatorial Kelvin wave further enhances this moisture transport, favoring convection in the region and initiating a cycle of the QBZD (146). Some evidence exists of QBZD activity being enhanced at the start of the African monsoon season when the ITCZ is closest to the equator (146), but more studies are needed to fully understand the relationship between the QBZD, Kelvin waves, and African monsoon onset.

The second dominant mode in 10–30-day filtered OLR over central and west Africa is a westward-propagating mode (147), referred to as the Sahelian mode owing to the latitude of the westward-propagating Rossby gyres (148). This mode appears over central Africa, propagates north to the Sahelian latitudes, and then moves west into the eastern Atlantic. It may also be associated with the west-east mode observed over the IAS (124), discussed in Section 2.2.2. Studies suggest that feedback from modulation of surface heat fluxes by rainfall can produce intraseasonal variability in rainfall on 10–30-day timescales (149). The Sahelian mode appears to be a combination of a meridional mode 1 and 2 ER wave forced by localized diabatic heating and land surface interactions (144). Upscale feedback associated with synoptic transients may also play a role in establishing westward-propagating convective anomalies on these timescales over west Africa (150, 151) and are discussed next.

African easterly waves (AEWs): tropical depression-type waves over Africa

2.4.3. Higher-frequency variability. Synoptic variability in African monsoon rainfall during northern summer is dominated by African easterly waves (AEWs) (32, 33, 40). This activity is found to be sensitive to the strength of the African easterly jet (AEJ), vertical shear, and the spatial extent of the potential vorticity reversal, which is a source of energy to the waves (34, 35, 151, 152). Some recent studies of AEWs suggest that the dynamic instabilities of the flow over west Africa are not sufficient to explain the initiation and growth of AEWs and that a finite amplitude initial disturbance is required (153). One source of these initiating disturbances appears to come from MCS development over the mountains of Darfur near the entrance to the AEJ (32, 34, 35). Zonal differences in the variability in convection over central and east Africa from that over west Africa on intraseasonal timescales (144) suggest that enhancement of AEW activity results from a complex interaction between the intraseasonal variability of the AEJ and those of MCS development over Darfur (35). As discussed in the previous section, this interaction may have an internal mode of variability on intraseasonal timescales (151), which contributes to a 10–30-day periodicity in African monsoon rainfall.

Modulation of TD-type activity is observed in association with the 30–90-day African monsoon mode (25, 27), and upscale impacts on the 30–90-day mode have also been suggested (27), similar to what has been proposed for the Indo-Pacific basin (59). In addition, TC activity in the Atlantic main development region (MDR) is also modulated on 10–30-day and 30–90-day time periods (27, 154). Overall, this activity is well correlated with African monsoon convection when mean conditions in the MDR are favorable for cyclogenesis. However, when conditions in the MDR are less favorable to cyclogenesis, AEWs play a more important role in modulating Atlantic TC activity (2).

Kelvin wave activity on 6–7-day timescales has already been described in association with both the QBZD and 30–90-day modes over Africa. The large zonal wavelength of these disturbances (8,000 km) results in modulation of rainfall over all of west Africa with comparable magnitude to TD-type disturbances in this region (155). However, although TD-type activity is at a maximum during July and August, Kelvin wave activity tends to be at a maximum outside of the northern summer season when the ITCZ is closest to the equator (155, 156). In addition, Kelvin waves tend to be particularly active when an easterly vertical wind shear and enhanced moist anomalies associated with MJO convection are present over this region (157). The interaction of Kelvin waves and AEWs has also been implicated in cyclogenesis (158). Much of the Kelvin wave activity over Africa appears to initiate over the eastern Pacific and Amazonia and consists of wave packets rather than wave trains (155, 159). The reasons for this are largely unexplored, and the intermittency is consistent with these disturbances not being a dominant mode of African monsoon rainfall variability but rather playing a supporting role to the dominant lower-frequency modes.

Solar cycle: a periodic change in the sun's activity and appearance over about an 11-year cycle

Aerosol optical thickness (AOT): a measure of the degree to which aerosols reduce the transparency of the atmosphere to incoming solar radiation

Saharan dust layer: a warm, dry, dust-laden air layer originating over the Sahara and extending westward over the Atlantic Ocean

2.5. Atmospheric Transport

In addition to its impacts on the global weather and climate (19, 160), the MJO can also affect the atmospheric chemical composition, such as ozone, aerosols, carbon monoxide (CO) and carbon dioxide (CO_2), as summarized in a recent review (161). This subsection mainly discusses new findings since that review.

Ozone is one of the most important trace gases in the atmosphere, and about 90% of the total column ozone (TCO) resides in the stratosphere. The TCO intraseasonal anomalies are $\sim\pm 10$ Dobson units, which are comparable to the TCO variability on annual and interannual timescales associated with ENSO, the quasi-biennial oscillation, and the solar cycle (162). The MJO affects the TCO mainly through its influence on the vertical movement of the tropopause (162). The partial ozone intraseasonal anomalies maximize in or near the lower stratosphere between 30 and 200 hPa and account for more than 50% of the TCO anomalies (163). The TCO intraseasonal anomalies are mainly observed over the Pacific and Eastern Hemisphere and extend from the subtropics to the northern extratropics (north of 30°N) and the Arctic (162, 164).

The MJO also modulates the tropospheric ozone, about 10% of the TCO, especially near the equator (165, 166). It was found that the equatorial tropospheric column ozone (165), as well as the equatorial upper tropospheric ozone (166), decreases during the enhanced phase of MJO events. This indicates that MJO-related convection can directly impact the equatorial tropospheric column ozone and upper tropospheric ozone through direct convective mixing. That is, convection lifts the ozone-poor lower tropospheric air upward to the upper troposphere and decreases upper tropospheric ozone and the overall tropospheric column ozone.

The MJO can also affect aerosol concentrations and their spatial and temporal distributions (167–173). The first study of this nature (167) found large MJO-related aerosol optical thickness (AOT) anomalies over the equatorial Indian, western Pacific, and tropical Atlantic Oceans. Although the results from this study (167) are strongly dependent on which satellite aerosol product is used and are inconclusive, they have motivated many follow-on studies to show the far-reaching effect of the MJO on the global aerosol distribution. For example, over the tropical Atlantic, the MJO accounted for about 25% of the total AOT variance, and the MJO-related AOT anomalies are likely produced by MJO-related low-level zonal wind anomalies (168). When enhanced MJO convection is located over the equatorial Indian Ocean (western Pacific), persistent low-level westerly (easterly) anomalies over the equatorial Atlantic can suppress (enhance) the background trade winds that can cause the negative (positive) AOT anomalies over the Atlantic region (168). Consistent with this hypothesis, dust associated with the Saharan dust layer is the main aerosol type of the MJO-related aerosol anomalies over the tropical Atlantic (169). In a related study (170), observational and reanalysis data sets suggest that TD-type disturbances dominate aerosol spatial distributions over the tropical Atlantic. Over the Maritime Continent, the MJO modulates when visible burning is detectable (171). In the remote marine boundary layer over the Indian Ocean, MJO-associated convection strongly affects the local aerosol concentration because increased vertical mixing introduces new particles into the marine boundary layer, rainout clears the atmosphere of submicrometer aerosol particles, and high winds enhance the concentration of sea-salt aerosol particles in the local atmosphere (172). In Santiago, Chile, during boreal summer months, it was found that surface particulate matter (PM_{10}) concentrations vary by the phase of the MJO (173).

The MJO can also impact the atmospheric CO_2 concentration (174). The peak-to-peak amplitude of the composite MJO modulation of tropical midtropospheric CO_2 is ~1 ppmv, with a standard error of the composite mean <0.1 ppmv. The correlation structure for CO_2, rainfall, and vertical velocity indicates that positive (negative) anomalies in CO_2 arise because of upward (downward) large-scale vertical motions in the lower troposphere associated with the MJO.

3. REPRESENTATION OF MULTISCALE INTERACTIONS IN NUMERICAL MODELS

A long history exists in examining general circulation model (GCM) fidelity in representing tropical disturbances and CCEWs. Comprehensive reviews of these efforts have been published (1, 6, 175). Here, we emphasize recent activities in modeling TISV modes using regional models as well as improvements in GCMs, emphasizing the models' ability to capture not only the disturbances themselves but also their interactions on intraseasonal timescales.

3.1. Regional Models

Limited studies exist on evaluation of tropical waves in regional model simulations. Tulich et al. (176) examined convectively coupled Kelvin waves and TD-type disturbances in simulations of the global tropics using the Weather Research and Forecasting (WRF) model. Although both the observed horizontal phase speeds and three-dimensional structures of these two CCEWs were qualitatively well captured by the WRF model, significant biases were noted in the amplitude of model wave activity. TD-type disturbances are generally too active over the Indian Ocean and western Pacific warm pool region compared to gridded observations, and such disturbances might be responsible for too frequent TC genesis in these regions. In contrast, the amplitude of Kelvin wave activity is largely underestimated throughout the global tropics in this model. The authors note that convection in the WRF model is too strongly coupled to rotational circulation anomalies, which appears to be linked to the model's tendency to produce too much rain at off-equatorial latitudes, and leads to a double-ITCZ problem common in climate models. Similar model biases are also evident in other models (5).

Using the regional ocean-atmosphere coupled model developed by Wang et al. (177, 178), Rydbeck et al. (120) and Small et al. (179) examined the roles of remote forcing associated with the Indo-Pacific MJO and local feedbacks, including air-sea interactions for regulating the eastern Pacific MJO during the boreal summer. When the atmospheric component of this regional model was forced by lateral boundary conditions from gridded observations, intraseasonal variability and the coupling between convection and winds were well simulated. However, when intraseasonal disturbances propagated into the domain were removed at the boundaries, eastern Pacific intraseasonal variability collapsed. These results differ from those obtained using a GCM (120) in which realistic eastern Pacific intraseasonal variability could be sustained even when the eastern Pacific was isolated from western Pacific intraseasonal forcing. Hence, the ability to sustain the eastern Pacific MJO through purely local processes appeared to be model dependent. It was argued that the regional model could not sustain MJO activity through purely local processes because surface wind–evaporation feedbacks that were previously proposed to be critical for supporting the eastern Pacific MJO (75) were unrealistically weak owing to model mean state easterly biases (120). Ocean-atmosphere coupling was found to have only a small effect on the eastern Pacific MJO.

Hagos et al. (180) used a moisture-nudged regional model to demonstrate that a realistic MJO heating structure, including development of a stratiform component, could only be maintained with a realistic evolution of the moisture field. In particular, low-level moistening during the onset stage of the MJO and upper-level moistening after the peak of MJO convection are crucial to a realistic MJO simulation.

Gross moist stability: the advective export of moist static energy from the atmospheric column per unit of convective activity

Convective momentum transport: the exchange of momentum between the cloud and environment typically associated with vertical cloud motions

3.2. Global Models

Because faithful simulation of TISV modes still presents a great challenge for global models (6), sensitivity of TISV to model parameterizations, particularly in convective schemes, has been extensively explored. Lin et al. (181) illustrated that increases in the strength of the convective triggering can lead to general improvements in simulating TISV, including more coherent eastward propagation of the MJO and reduced propagation speed of CCEWs. One hypothesis is that the changes in phase speed in the simulated CCEWs are associated with a change of the gross moist stability of the atmosphere (181, 182). This group also found that adding a moisture trigger in the mass flux convective scheme could also have positive impacts on the vertical tilt of simulated Kelvin waves (182).

For MJO simulations, Zhou et al. (183) found that significant improvements can be achieved in the Community Climate System Model 4 (CCSM4) by considering a dilute plume approximation and an implementation of convective momentum transport in the deep convection scheme. Inclusion of the dilute plume approximation tends to make MJO temperature and convective heating anomalies more positively correlated, which supports available potential energy generation, whereas the inclusion of convective momentum transport improves the model MJO through better simulation of the mean low-level zonal winds over the Indian Ocean and western Pacific. On the basis of numerical experiments in hindcast mode, Holloway et al. (184) also showed that increased generation of available potential energy and its conversion into eddy kinetic energy in models can lead to a more realistic model MJO. Improvements in the simulated MJO with increasing convective entrainment and stronger moisture triggers have also been documented in other recent studies (185–188). These studies argued that increasing convective sensitivity to free tropospheric moisture leads to a more realistic MJO. Models with stronger variability tend to have reduced gross moist stability. This and other evidence for the critical importance of moisture to the MJO have led recent modeling studies to hypothesize that the MJO is a class of disturbance called a moisture mode (189–191). Other new global modeling studies have further shown that multiscale interactions between the MJO, synoptic, and mesoscale disturbances are important to the moisture and momentum budgets of the MJO (190, 192, 193).

Simulations of TISV have been comprehensively explored in GCMs participating in the Intergovernmental Panel on Climate Change (IPCC) climate assessment reports. Lin et al. (175) evaluated the MJO and CCEWs in 14 GCMs of the Coupled Model Intercomparison Project Phase 3 (CMIP3), model data sets created in support of the fourth IPCC report released in 2007. It was found that the 2–128-day band-pass filtered precipitation variance is too weak in most of the models and that only 2 out of the 14 models realistically simulated observed MJO variance. About half of the models capture signals of CCEWs, with particularly strong Kelvin and MRG-EIG wave signals. However, the variance of the CCEWs is too weak for all of these modes except the EIG wave. In addition, phase speeds of the CCEWs tend to be faster than in the gridded observations.

As an extension of the study of Lin et al. (175), Straub et al. (194) performed a detailed analysis of coupled Kelvin wave activity and its three-dimensional structures in 20 CMIP3 GCMs. They found that only 5 of the 20 models captured Kelvin wave activity distributions and wave structures that resemble the observations. Most of the models exhibit large deficiencies in lower-tropospheric temperature and humidity signals near the location of maximum precipitation, suggesting the lack of a self-suppression mechanism of deep convection in these models, which was also discussed by

Lin et al. (175). These second vertical baroclinic structures in temperature and humidity could be critical in generating Kelvin waves, as was proposed by the stratiform-instability mechanism (63, 195, 196). Straub et al. (194) also suggested that models with convective adjustment–type cumulus schemes generally exhibit less success at representing Kelvin waves. In general, most CMIP3 models simulate westward propagation of TD-type waves relatively well but produce relatively poor eastward propagation of the MJO and variance too weak for either the TD-type waves or MJO (181).

Superparameterized: a global climate model with a two-dimensional cloud-resolving model embedded within each grid

Although simulating TISV in climate models is still a challenge, recent studies demonstrate that the newer CMIP5 models that are part of the fifth IPCC report released in 2013 exhibit an overall improvement over the CMIP3 models in the simulation of the MJO and several CCEWs (6). Intraseasonal (2–128-day) variance of precipitation is higher than in the CMIP3 models, with stronger variance of Kelvin, ER, and EIG waves. Although only half of the CMIP3 models were able to represent the signature of the CCEWs (175), almost all CMIP5 models can simulate CCEWs to varying degrees. This is especially true for the Kelvin and the MRG-EIG waves. Moreover, the equivalent depth of the waves, which is a measure of the coupling between convection and circulation, is more realistically captured in CMIP5 models.

Jiang et al. (197) examined model fidelity in representing leading TISV modes over the eastern Pacific in nine GCMs, including one superparameterized community atmosphere model (SPCAM) and one high-resolution GCM [the Geophysical Fluid Dynamics Laboratory High-Resolution Atmospheric Model (HiRAM)] with a horizontal resolution of about 50 km. A few of the GCMs reasonably capture the evolution patterns of either the MJO or the east Pacific 10–30-day mode. Only two models, SPCAM and HiRAM, show the ability to simulate both of the two leading TISV modes. Although the simulation in SPCAM might benefit from its explicit representation of cumulus processes, the improved representation in HiRAM could be attributed to the employment of a strongly entraining plume cumulus scheme and fine horizontal resolution. An additional experiment with HiRAM, but with a coarse resolution, supports the hypothesis that increased horizontal resolution tends to be essential to resolve the 20-day north-south mode over the eastern Pacific, but it does not significantly affect the MJO mode in this basin.

A noteworthy finding from Jiang et al. (197) was that, even though a strong link between eastward-propagating MJO signals from the western Pacific and the MJO mode over the eastern Pacific is evident in the observations, this linkage is not evident in several GCMs that exhibit a realistic MJO mode over the eastern Pacific. The convective signals associated with the MJO mode in these models tend to originate over the equatorial central Pacific between 150°E and 150°W. This may suggest that the MJO mode over the eastern Pacific could be self-sustained without a forcing from the eastward-propagating MJO. This notion was further confirmed by recent model studies (120, 198). As alluded to in Section 3.1, a numerical experiment with a GCM in which an equatorial sponge region in the central Pacific isolates the eastern Pacific from the western Pacific produces as realistic a simulation of the eastern Pacific MJO as in the control run without a sponge region, although phase locking in MJO activity between hemispheres is broken owing to the lack of an equatorial communication pathway (120).

Model performance in capturing the leading eastern Pacific TISV modes during the boreal summer was also examined in 16 CMIP5 GCMs by Jiang et al. (198). Among the 16 GCMs, only 7 capture the spatial pattern of the eastern Pacific MJO (the leading mode TISV mode) relatively well, although even these GCMs exhibit biases in simulating the MJO amplitude. Analyses indicate that model fidelity in representing the eastern Pacific MJO is closely associated with the ability to simulate a realistic summer mean state. The presence of westerly or weak mean easterly winds over the eastern Pacific warm pool region as in the observations was hypothesized to be important for realistic simulations of the MJO by producing the correct sign of surface flux anomalies relative to the MJO convection that helps to destabilize local intraseasonal disturbances. Jiang et al. (198) also noted that several GCMs that can simulate the MJO over the eastern Pacific relatively well show poor MJO simulations for the Indian Ocean and western Pacific. These results suggest that, in addition to model cumulus parameterizations, other factors, such as a realistic mean state, may also be crucial for faithful simulations of the regional features of intraseasonal variability.

TD-type activity in CMIP5 models has also been examined in the eastern Pacific (199). The multimodel mean track density based on nine models generally agrees well with that from reanalysis, but the ability of any one model to capture this parameter varies widely. For mean wave strength, the observed eastern Pacific maximum along the coast of Mexico is reasonably well captured in the multimodel mean pattern; however, this strength is strongly underestimated in the Gulf of Mexico and along the east coast of the United States. Unlike track density, this bias is common to most models. Limitations as a result of coarse model resolution may degrade the simulation of mean strength. In addition, like CMIP3 models, CMIP5 models exhibit a cold bias in the Gulf of Mexico and the tropical-subtropical west Atlantic, potentially reducing the frequency and strength of TCs in these regions (200). Large values in wave strength are strongly biased toward regions of TC activity and are thus more likely to be affected by SST biases than track density. The SST bias may also be linked to the models' tendency to overestimate the strength of the CLLJ (200).

4. FORECASTING AND SEASONAL PREDICTION

4.1. Predictive Skill for the Madden-Julian Oscillation

As one of the primary sources for short-term climate predictability, forecasting the MJO has attracted great interest in the climate research community in recent decades (201). However, until recently, the useful predictive forecasts of the MJO had generally been limited to only one to two weeks (181, 202, 203). Improvements in model physics, spatial resolution, and data assimilation systems have led to significant increases in the predictive forecasts of the MJO in a few models. For example, the European Centre for Medium-Range Weather Forecasts' (ECMWF) Integrated Forecast System (IFS) (204), the National Centers for Environmental Prediction Climate Forecast System (205–207), and the Predictive Ocean-Atmosphere Model for Australia (208) produce useful TISV predictive forecasts out to two to four weeks. In a recent analysis by Mani et al. (209), the predictability of the MJO was explored by evaluating the divergence in ensemble member hindcasts from eight different coupled models participating in the Intraseasonal Variability Hindcast Experiment. MJO predictability of three to four weeks was obtained from most of the models examined. The models' hindcast skill was generally less than the estimated potential predictability limits by about one week, suggesting that more skillful MJO forecasts can be afforded through further improvements of dynamical models. Studies have shown that improving the moist physical parameterization of models, particularly the sensitivity of convection to free tropospheric humidity, can lead to significant improvements in MJO forecasts (210–213).

4.2. Tropical Cyclone Intraseasonal Prediction

Owing to the intimate relationships between modes of TISV and higher-frequency disturbances, including TCs and TD-type waves (20, 83, 84), TISV provides the physical basis to justify efforts to forecast these higher-frequency disturbances on intraseasonal timescales. For intraseasonal prediction of TC activity, owing to the traditionally limited predictive skill for the MJO in climate models, statistical models have often outperformed dynamical models (201, 214). Moreover, most of the current global climate models use too coarse of a horizontal resolution to resolve TC scales of motion. This is one of the main reasons that intraseasonal TC prediction efforts have relied heavily on statistical approaches (55, 81, 86).

With the recently improved ability to capture TISV in numerical models, along with the finer resolutions that can better resolve TCs, numerical models are becoming increasingly useful tools in intraseasonal TC forecasts. For example, Vitart (82) used the ECMWF IFS with a horizontal resolution of 80 km to illustrate for the first time that it is possible for a conventional global model to represent both TISV and TCs and their intimate relationships. Jiang et al. (85) illustrated that the observed dominant TISV modes over the eastern Pacific and their strong modulation of TCs are well simulated in a HiRAM atmosphere-only run. Inspired by these encouraging modeling achievements, enthusiasm in the community has grown for exploring dynamical TC forecasts on intraseasonal timescales (204, 215–217). For example, Vitart et al. (204) evaluated the skill of the ECMWF IFS to predict the occurrence of TCs over the Southern Hemisphere out to three weeks and compared it to the skill of a statistical model (81). Vitart et al. (204) showed that the ECMWF hindcasts have higher "hit" rates relative to false alarm rates than the statistical model for the first three weeks of integrations. After a simple calibration of the total TC numbers in the ECMWF forecasts, the calibrated dynamical model also has higher skill relative to climatology than the statistical model during the first three weeks.

5. DISCUSSION AND CONCLUSIONS

The past decade has provided many interesting and important insights into TISV. For example, the isolation of ER modes over Africa has contributed to our understanding of the complex relationship between the Asian and African monsoons. It has also revealed the physical mechanism establishing the dominant mode of African monsoon variability, distinguishing it from the Asian monsoon, which is dominated by the lower-frequency MJO and BSISO modes. The discovery of a north-south mode over the eastern Pacific, evidence that the eastern Pacific supports an independent MJO mode from that in the Indo-Pacific, and the potential relationship between the biweekly modes over Africa and those over the IAS have also contributed to a more complete understanding of TISV in the eastern Pacific. In addition, these discoveries have raised new questions regarding what physical mechanisms support these observed modes and how they might be exploited along with the more established modes of TISV to improve medium-range to seasonal forecasts throughout the tropics and midlatitudes. The apparent interconnectedness of the world's monsoons has important consequences for global climate to be further explored. Representation of the global monsoon system should also be a priority for climate models used in climate projections.

Despite the long history of studies on the Indo-Pacific MJO, many aspects of this mode require deeper investigation. Interactions between the MJO and higher-frequency disturbances, as they impact the momentum and moisture budgets and hence maintenance of the MJO, require continued study. The cyclic nature of the MJO makes it difficult to distinguish the necessary processes for the initiation of the MJO from preexisting MJO modulated processes. By examining primary Indo-Pacific MJO events, some progress has been made in better understanding MJO initiation (89, 90). However, different methods of defining the MJO can result in different precursor conditions being isolated. In addition, as suggested by recent field campaign observations (76), the roles of ER and Kelvin waves in Indo-Pacific MJO initiation need additional investigation, as does the role of extratropical Rossby waves with respect to MJO initiation and propagation.

In addition to recent progress on MJO dynamics, studies of MJO-related atmospheric transport provide a wealth of new information on the MJO's chemical impacts on the global climate system. However, many open questions exist regarding MJO-related atmospheric transport. For example, over the near-equatorial convective regions, can new and improved satellite tropospheric ozone data demonstrate that the MJO systematically influences tropospheric ozone? If so, what is the dynamic (convective transport) versus chemical (ozone production/destruction due to ozone precursors and lightning) contribution to the tropospheric ozone variations? Over the equatorial Indian and western Pacific Oceans, can new and improved satellite aerosol products, such as the Cloud-Aerosol Lidar and Infrared Pathfinder Satellite Observations (218), show that the MJO systematically influences aerosol concentrations? If so, what are the physical mechanisms for the aerosol variation in deep convection? These questions demand more studies of MJO-related ozone and aerosol variations using new and improved in situ, satellite, and data assimilation products, as well as chemical transport models that include aerosols. When fully described, socially relevant medium-range forecasts of atmospheric composition and air quality may be possible given the potential predictability of the MJO (201). In addition, intraseasonal atmospheric composition variations are useful tests for the performance of Earth system models.

Representation of TISV in numerical models has shown notable improvement, although challenges remain in representing convective processes, including mesoscale convective organization and its coupling to the larger scales over a global domain. Although important strides have been made in understanding the factors that contribute to improved simulation of TISV modes, the ability of these models to correctly simulate the multiscale processes involved in, for instance, interactions of MCSs with CCEWs and MJOs, and transitions between CCEW structures against a changing background flow, remains limited. The dependence of scale selection and wave growth on the background flow also highlights the importance of the models' mean state for realistic simulation of TISV. The interactions of TISV with both larger and smaller scales of variability suggest it remains a challenge to interpret future climate projections using the current generation of climate models, though a few models offer great promise in this respect. A charge for CMIP6 (219) is to address the question of how the links between weather and climate bridged by TISV might be altered by the evolving warming background state.

This review has focused on tropical and Northern Hemisphere TISV. The modes of variability on these timescales strongly interact with one another and with their environment, with both upscale and downscale feedbacks playing important roles in the life cycle and propagation characteristics of the modes. Although not discussed here in detail, these interactions also extend into the Southern Hemisphere, and a full understanding of TISV must include such interactions. TISV interactions with ENSO are also an important aspect of the global climate and require further studies (96). For example, studies suggest that a model's ability to correctly capture the MJO also improves its ability to capture ENSO (64). Mesoscale processes and their relationship to TISV, which were outside the scope of this review, must also be more fully explored to better understand the link between local weather and intraseasonal scale phenomena and to predict how these interactions will evolve within a changing climate.

DISCLOSURE STATEMENT

The authors are not aware of any affiliations, memberships, funding, or financial holdings that might be perceived as affecting the objectivity of this review.

ACKNOWLEDGMENTS

Y. Serra thanks National Science Foundation (NSF) and National Oceanic and Atmospheric Administration (NOAA) for their support under awards NSF AGS-0756806, NOAA CPPA NA06OAR4310057, and NOAA MAPP NA10OAR4310167. X. Jiang acknowledges support by NSF under award AGS-1228302, and the NOAA MAPP program under award NA12OAR4310075. Part of the research for this study was carried out at the Jet Propulsion Laboratory, California Institute of Technology, under a contract with the National Aeronautics and Space Administration. J. Amador thanks the following projects for their support: IAI-CRN2-050, UCR-VI-805-B0-065, A8-606, B0-130, A9-224, A7-002, B0-402, B3-600, and 808-A9-180. E. Maloney acknowledges support from the NOAA MAPP Project NA12OAR4310077 and NSF Grants AGS-1347738 and AGS-0946911.

LITERATURE CITED

1. Kiladis GN, Wheeler MC, Haertel PT, Straub KH, Roundy PE. 2009. Convectively coupled equatorial waves. *Rev. Geophys.* 47(2):RG2003
2. Moncrieff MW, Waliser DE, Caughey J. 2012. Progress and direction in tropical convection research: YOTC International Science Symposium. *Bull. Am. Meteorol. Soc.* 93(8):ES65–69
3. Kiladis GN, Weickmann KM. 1997. Horizontal structure and seasonality of large-scale circulations associated with submonthly tropical convection. *Mon. Weather Rev.* 125(9):1997–2013
4. Matthews AJ, Kiladis GN. 1999. The tropical-extratropical interaction between high-frequency transients and the Madden-Julian Oscillation. *Mon. Weather Rev.* 127(5):661–77
5. Yang G-Y, Slingo J, Hoskins B. 2009. Convectively coupled equatorial waves in high-resolution Hadley Centre climate models. *J. Clim.* 22(8):1897–919
6. Hung M-P, Lin J-L, Wang W, Kim D, Shinoda T, Weaver SJ. 2013. MJO and convectively coupled equatorial waves simulated by CMIP5 climate models. *J. Clim.* 26(17):6185–214
7. Riehl H. 1945. *Waves in the Easterlies and the Polar Front in the Tropics*. Chicago: Univ. Chicago Press
8. Matsuno T. 1966. Quasi-geostrophic motions in the equatorial area. *J. Meteorol. Soc. Jpn.* 44(1):25–42
9. Takayabu YN. 1994. Large-scale cloud disturbances associated with equatorial waves. Part I: Spectral features of the cloud disturbances. *J. Meteorol. Soc. Jpn.* 72(3):433–49
10. Takayabu YN. 1994. Large-scale cloud disturbances associated with equatorial waves. Part II: Westward-propagating inertio-gravity waves. *J. Meteorol. Soc. Jpn.* 72:451–65
11. Wheeler M, Kiladis GN. 1999. Convectively coupled equatorial waves: analysis of clouds and temperature in the wavenumber-frequency domain. *J. Atmos. Sci.* 56(3):374–99
12. Holton JR, Lindzen RS. 1972. An updated theory for the quasi-biennial cycle of the tropical stratosphere. *J. Atmos. Sci.* 29(6):1076–80
13. Wallace JM, Chang LA. 1972. On the application of satellite data on cloud brightness to the study of tropical wave disturbances. *J. Atmos. Sci.* 29(7):1400–3
14. Gruber A. 1974. The wavenumber-frequency spectra of satellite-measured brightness in the tropics. *J. Atmos. Sci.* 31(6):1675–80
15. Zangvil A. 1975. Temporal and spatial behavior of large-scale disturbances in tropical cloudiness deduced from satellite brightness data. *Mon. Weather Rev.* 103(10):904–20
16. Madden RA, Julian PR. 1971. Detection of a 40–50 day oscillation in the zonal wind in the tropical Pacific. *J. Atmos. Sci.* 28:702–8
17. Madden RA, Julian PR. 1972. Description of global-scale circulation cells in the tropics with a 40–50 day period. *J. Atmos. Sci.* 29(6):1109–23
18. Hendon HH, Salby ML. 1994. The life cycle of the Madden-Julian oscillation. *J. Atmos. Sci.* 51(15):2225–37
19. Lau WKM, Waliser DE, eds. 2012. *Intraseasonal Variability in the Atmosphere-Ocean Climate System*. Heidelberg, Ger.: Springer. 2nd ed.
20. Maloney E, Hartmann D. 2000. Modulation of eastern North Pacific hurricanes by the Madden-Julian oscillation. *J. Clim.* 13(9):1451–60
21. Mo KC. 2000. Intraseasonal modulation of summer precipitation over North America. *Mon. Weather Rev.* 128:1490–505
22. Maloney ED, Hartmann DL. 2001. The Madden-Julian oscillation, barotropic dynamics, and North Pacific tropical cyclone formation. Part I: Observations. *J. Atmos. Sci.* 58(17):2545–58

23. Kikuchi K, Wang B. 2010. Formation of tropical cyclones in the northern Indian Ocean associated with two types of tropical intraseasonal oscillation modes. *J. Meteorol. Soc. Jpn.* 88(3):475–96
24. Klotzbach PJ. 2014. The Madden-Julian oscillation's impacts on worldwide tropical cyclone activity. *J. Clim.* 27:2317–30
25. Matthews A. 2004. Intraseasonal variability over tropical Africa during northern summer. *J. Clim.* 17(12):2427–40
26. Lorenz DJ, Hartmann DL. 2006. The effect of the MJO on the North American monsoon. *J. Clim.* 19:333–43
27. Maloney ED, Shaman J. 2008. Intraseasonal variability of the west African monsoon and Atlantic ITCZ. *J. Clim.* 21(12):2898–918
28. Pai DS, Bhate J, Sreejith OP, Hatwar HR. 2009. Impact of MJO on the intraseasonal variation of summer monsoon rainfall over India. *Clim. Dyn.* 36(1–2):41–55
29. McPhaden MJ. 1999. Genesis and evolution of the 1997–98 El Niño. *Science* 283(5404):950–54
30. Vecchi GA, Harrison DE. 2000. Tropical Pacific sea surface temperature anomalies, El Niño, and equatorial westerly wind events. *J. Clim.* 13:1814–30
31. Vecchi GA, Harrison DE. 2003. On the termination of the 2002–03 El Niño event. *Geophys. Res. Lett.* 30(18):1964
32. Burpee RW. 1972. The origin and structure of easterly waves in the lower troposphere of North Africa. *J. Atmos. Sci.* 29:77–90
33. Norquist DC, Recker EE, Reed RJ. 1977. The energetics of African wave disturbances as observed during phase III of GATE. *Mon. Weather Rev.* 105(3):334–42
34. Kiladis GN, Thorncroft C, Hall N. 2006. Three-dimensional structure and dynamics of African easterly waves. *J. Atmos. Sci.* 63:2212–30
35. Thorncroft CD, Hall N, Kiladis GN. 2008. Three-dimensional structure and dynamics of African easterly waves. Part III: Genesis. *J. Atmos. Sci.* 65(11):3596–607
36. Reed RJ, Recker EE. 1971. Structure and properties of synoptic-scale wave disturbances in the equatorial western Pacific. *J. Atmos. Sci.* 28(7):1117–33
37. Nitta T, Takayabu Y, Nakagomi Y, Suzuki Y, Hasegawa N, Kadokura A. 1985. Global analysis of the lower tropospheric disturbances in the tropics during the northern summer of the FGGE year. Part I: Global features of the disturbances. *J. Meteorol. Soc. Jpn.* 63:1–19
38. Takayabu YN, Nitta T. 1993. 3–5 day-period disturbances coupled with convection over the tropical Pacific ocean. *J. Meteorol. Soc. Jpn.* 71(2):221–46
39. Dunkerton TJ, Baldwin MP. 1995. Observation of 3–6-day meridional wind oscillations over the tropical Pacific, 1973–1992: horizontal structure and propagation. *J. Atmos. Sci.* 52(10):1585–601
40. Roundy P, Frank W. 2004. A climatology of waves in the equatorial region. *J. Atmos. Sci.* 61(17):2105–32
41. Shapiro LJ. 1986. The three-dimensional structure of synoptic-scale disturbances over the tropical Atlantic. *Mon. Weather Rev.* 114:1876–91
42. Serra YL, Kiladis GN, Cronin MF. 2008. Horizontal and vertical structure of easterly waves in the Pacific ITCZ. *J. Atmos. Sci.* 65(4):1266–84
43. Ferreira RN, Schubert WH. 1997. Barotropic aspects of ITCZ breakdown. *J. Atmos. Sci.* 54(2):261–85
44. Molinari J, Knight D, Dickinson M, Vollaro D, Skubis S. 1997. Potential vorticity, easterly waves, and eastern Pacific tropical cyclogenesis. *Mon. Weather Rev.* 125(10):2699–708
45. Wang C-C, Magnusdottir G. 2006. The ITCZ in the central and eastern Pacific on synoptic time scales. *Mon. Weather Rev.* 134(5):1405–21
46. Serra YL, Kiladis GN, Hodges KI. 2010. Tracking and mean structure of easterly waves over the Intra-Americas Sea. *J. Clim.* 23(18):4823–40
47. Méndez M, Magaña V. 2010. Regional aspects of prolonged meteorological droughts over Mexico and Central America. *J. Clim.* 23(5):1175–88
48. Toma VE, Webster PJ. 2010. Oscillations of the intertropical convergence zone and the genesis of easterly waves. Part I: Diagnostics and theory. *Clim. Dyn.* 34(4):587–604
49. Toma VE, Webster PJ. 2010. Oscillations of the intertropical convergence zone and the genesis of easterly waves. Part II: Numerical verification. *Clim. Dyn.* 34(4):605–13

50. Lau K-H, Lau N-C. 1992. The energetics and propagation dynamics of tropical summertime synoptic-scale disturbances. *Mon. Weather Rev.* 120:2523–39
51. Sobel AH, Bretherton CS. 1999. Development of synoptic-scale disturbances over the summertime tropical northwest Pacific. *J. Atmos. Sci.* 56(17):3106–27
52. Raymond DDJ, López-Carrillo C, Cavazos LL. 1998. Case-studies of developing east Pacific easterly waves. *Q. J. R. Meteorol. Soc.* 124(550):2005–34
53. Zehnder JA, Powell DM, Ropp DL. 1999. The interaction of easterly waves, orography, and the intertropical convergence zone in the genesis of eastern Pacific tropical cyclones. *Mon. Weather Rev.* 127(7):1566–85
54. Molinari J, Vollaro D, Skubis S, Dickinson M. 2000. Origins and mechanisms of eastern Pacific tropical cyclogenesis: a case study. *Mon. Weather Rev.* 128(1):125–39
55. Frank WM, Roundy PE. 2006. The role of tropical waves in tropical cyclogenesis. *Mon. Weather Rev.* 134:2397–417
56. Holland GJ. 1995. Scale interaction in the western Pacific monsoon. *Meteorol. Atmos. Phys.* 56:57–79
57. Ritchie EA, Holland GJ. 1999. Large-scale patterns associated with tropical cyclogenesis in the western Pacific. *Mon. Weather Rev.* 127(9):2027–43
58. Maloney E, Dickinson M. 2003. The intraseasonal oscillation and the energetics of summertime tropical western North Pacific synoptic-scale disturbances. *J. Atmos. Sci.* 60(17):2153–68
59. Straub KH, Kiladis GN. 2003. Interactions between the boreal summer intraseasonal oscillation and higher-frequency tropical wave activity. *Mon. Weather Rev.* 131(5):945–60
60. Dunkerton TJ, Montgomery MT, Wang Z. 2009. Tropical cyclogenesis in a tropical wave critical layer: easterly waves. *Atmos. Chem. Phys.* 9(15):5587–646
61. Wheeler MC, McBride JL. 2012. Australasian monsoon. See Ref. 19, pp. 147–97
62. Carvalho LMV, Silva AE, Jones C, Liebmann B, Silva Dias PL, Rocha HR. 2010. Moisture transport and intraseasonal variability in the South America monsoon system. *Clim. Dyn.* 36(9–10):1865–80
63. Khouider B, Majda AJ. 2008. Equatorial convectively coupled waves in a simple multicloud model. *J. Atmos. Sci.* 65:3376–97
64. Zhang C. 2013. Madden-Julian oscillation: bridging weather and climate. *Bull. Am. Meteorol. Soc.* 94(12):1849–70
65. Roundy PE. 2012. Tropical-extratropical interactions. See Ref. 19, pp. 497–512
66. Simpson J, Adler RF, North GR. 1988. A proposed Tropical Rainfall Measuring Mission (TRMM) satellite. *Bull. Am. Meteorol. Soc.* 69(3):278–95
67. Chahine MT, Pagano TS, Aumann HH, Atlas R. 2006. AIRS: improving weather forecasting and providing new data on greenhouse gases. *Bull. Am. Meteorol. Soc.* 87(7):911–26
68. L'Ecuyer TS, Jiang JH. 2010. Touring the atmosphere aboard the A-Train. *Phys. Today* 63:36–41
69. Moncrieff MW, Waliser DE, Miller MJ, Shapiro MA, Asrar GR, Caughey J. 2012. Multiscale convective organization and the YOTC virtual global field campaign. *Bull. Am. Meteorol. Soc.* 93(8):1171–87
70. Parkinson CL. 2013. Summarizing the first ten years of NASA's Aqua Mission. *IEEE J. Sel. Top. Appl. Earth Obs. Remote Sens.* 6(3):1179–88
71. Black PG, D'Asaro EA, Sanford TB, Drennan WM, Zhang JA, et al. 2007. Air-sea exchange in hurricanes: synthesis of observations from the Coupled Boundary Layer Air-Sea Transfer Experiment. *Bull. Am. Meteorol. Soc.* 88(3):357–74
72. Yoneyama K, Zhang C, Long CN. 2013. Tracking pulses of the Madden-Julian oscillation. *Bull. Am. Meteorol. Soc.* 94:1871–91
73. Dee DP, Uppala SM, Simmons AJ. 2011. The ERA interim reanalysis: configuration and performance of the data assimilation system. *Q. J. R. Meteorol. Soc.* 137:553–97
74. Nakazawa T. 1988. Tropical super clusters within intraseasonal variations over the western Pacific. *J. Meteorol. Soc. Jpn.* 66(6):823–39
75. Maloney E, Esbensen S. 2003. The amplification of east Pacific Madden-Julian oscillation convection and wind anomalies during June-November. *J. Clim.* 16(21):3482–97
76. Gottschalck J, Roundy PE, Schreck CJ III, Vintzileos A, Zhang C. 2013. Large-scale atmospheric and oceanic conditions during the 2011–12 DYNAMO field campaign. *Mon. Weather Rev.* 141(12):4173–96

77. Houze RA. 2004. Mesoscale convective systems. *Rev. Geophys.* 42(4):RG4003
78. Hsu H-H, Hoskins BJ, Jin F-F. 1990. The 1985/86 intraseasonal oscillation and the role of the extra-tropics. *J. Atmos. Sci.* 47(7):823–39
79. Hsu H-H, Weng C-H, Wu C-H. 2004. Contrasting characteristics between the northward and eastward propagation of the intraseasonal oscillation during the boreal summer. *J. Clim.* 17(4):727–43
80. Jiang X, Lau N-C. 2008. Intraseasonal teleconnection between North American and western North Pacific monsoons with 20-day time scale. *J. Clim.* 21(11):2664–79
81. Leroy A, Wheeler MC. 2008. Statistical prediction of weekly tropical cyclone activity in the Southern Hemisphere. *Mon. Weather Rev.* 136(10):3637–54
82. Vitart F. 2009. Impact of the Madden Julian Oscillation on tropical storms and risk of landfall in the ECMWF forecast system. *Geophys. Res. Lett.* 36:L15802
83. Klotzbach PJ. 2010. On the Madden-Julian Oscillation–Atlantic hurricane relationship. *J. Clim.* 23(2):282–93
84. Alaka GJ Jr, Maloney ED. 2012. The influence of the MJO on upstream precursors to African easterly waves. *J. Clim.* 25(9):3219–36
85. Jiang X, Zhao M, Waliser DE. 2012. Modulation of tropical cyclones over the eastern Pacific by the intraseasonal variability simulated in an AGCM. *J. Clim.* 25:6524–38
86. Slade SA, Maloney ED. 2013. An intraseasonal prediction model of Atlantic and east Pacific tropical cyclone genesis. *Mon. Weather Rev.* 141(6):1925–42
87. Roundy PE. 2012. Tracking and prediction of large-scale organized tropical convection by spectrally focused two-step space-time EOF analysis. *Q. J. R. Meteorol. Soc.* 138:919–31
88. Roundy PE. 2012. The spectrum of convectively coupled Kelvin waves and the Madden-Julian oscillation in regions of low-level easterly and westerly background flow. *J. Atmos. Sci.* 69(7):2107–11
89. Straub KH. 2013. MJO initiation in the real-time multivariate MJO index. *J. Clim.* 26(4):1130–51
90. Ling J, Zhang C, Bechtold P. 2013. Large-scale distinctions between MJO and non-MJO convective initiation over the tropical Indian Ocean. *J. Atmos. Sci.* 70(9):2696–712
91. Matthews AJ. 2008. Primary and successive events in the Madden-Julian Oscillation. *Q. J. R. Meteorol. Soc.* 134(631):439–53
92. Kemball-Cook SR, Weare BC. 2001. The onset of convection in the Madden-Julian oscillation. *J. Clim.* 14:780–93
93. Mo KC, Jones C, Paegle JN. 2012. Pan America. See Ref. 19, pp. 111–45
94. Guan B, Waliser DE, Molotch NP, Fetzer EJ, Neiman PJ. 2012. Does the Madden-Julian oscillation influence wintertime atmospheric rivers and snowpack in the Sierra Nevada? *Mon. Weather Rev.* 140(2):325–42
95. Yu W, Han W, Maloney ED, Gochis D. 2011. Observations of eastward propagation of atmospheric intraseasonal oscillations from the Pacific to the Atlantic. *J. Geophys. Res.* 116:D02101
96. Lau WKM. 2012. El Niño Southern Oscillation connection. See Ref. 19, pp. 297–334
97. Yasunari T. 1979. Cloudiness fluctuations associated with the Northern Hemisphere summer monsoon. *J. Meteorol. Soc. Jpn.* 57(3):227–42
98. Webster PJ, Magana VO, Palmer TN, Shukla J. 1998. Monsoons: processes, predictability, and the prospects for prediction. *J. Geophys. Res.* 103(C7):14451–510
99. Jiang X, Li T, Wang B. 2004. Structures and mechanisms of the northward propagating boreal summer intraseasonal oscillation. *J. Clim.* 17(5):1022–39
100. Prasanna V, Annamalai H. 2012. Moist dynamics of extended monsoon breaks over South Asia. *J. Clim.* 25(11):3810–31
101. Goswami BN. 2012. South Asian monsoon. See Ref. 19, pp. 21–72
102. Fu X, Wang B, Li T, McCreary J. 2003. Coupling between northward-propagating, intraseasonal oscillations and sea surface temperature in the Indian Ocean. *J. Atmos. Sci.* 60(15):1733–53
103. DeMott CA, Stan C, Randall DA. 2013. Northward propagation mechanisms of the boreal summer intraseasonal oscillation in the ERA-interim and SP-CCSM. *J. Clim.* 26:1973–92
104. Chen T-C, Chen J-M. 1993. The 10–20-day mode of the 1979 Indian monsoon: its relation with the time variation of monsoon rainfall. *Mon. Weather Rev.* 121(9):2465–82

105. Chang C-P, Chen GT-J. 1995. Tropical circulations associated with southwest monsoon onset and westerly surges over the South China Sea. *Mon. Weather Rev.* 123(11):3254–67
106. Wang B, Xu X. 1997. Northern Hemisphere summer monsoon singularities and climatological intraseasonal oscillation. *J. Clim.* 10(5):1071–85
107. Fukutomi Y, Yasunari T. 1999. 10–25 day intraseasonal variations of convection and circulation over East Asia and western North Pacific during early summer. *J. Meteorol. Soc. Jpn.* 77(3):753–69
108. Chen T-C, Yen M-C, Weng S-P. 2000. Interaction between the summer monsoons in East Asia and the South China Sea: intraseasonal monsoon modes. *J. Atmos. Sci.* 57(9):1373–92
109. Hartmann DL, Michelsen ML, Klein SA. 1992. Seasonal variations of tropical intraseasonal oscillations: a 20–25-day oscillation in the western Pacific. *J. Atmos. Sci.* 49(14):1277–89
110. Kemball-Cook S, Wang B. 2001. Equatorial waves and air-sea interaction in the boreal summer intraseasonal oscillation. *J. Clim.* 14(13):2923–42
111. Lawrence DM, Webster PJ. 2001. Interannual variations of the intraseasonal oscillation in the South Asian summer monsoon region. *J. Clim.* 14(13):2910–22
112. Joseph S, Sahai AK, Goswami BN. 2008. Eastward propagating MJO during boreal summer and Indian monsoon droughts. *Clim. Dyn.* 32(7–8):1139–53
113. Flatau MK, Flatau PJ, Schmidt J, Kiladis GN. 2003. Delayed onset of the 2002 Indian monsoon. *Geophys. Res. Lett.* 30(14):1768
114. Straub KH, Kiladis GN, Ciesielski PE. 2006. The role of equatorial waves in the onset of the South China Sea summer monsoon and the demise of El Niño during 1998. *Dyn. Atmos. Ocean.* 42(1–4):216–38
115. Webster PJ, Chang H-R. 1988. Equatorial energy accumulation and emanation regions: impacts of a zonally varying basic state. *J. Atmos. Sci.* 45(5):803–29
116. Chen G, Huang R. 2009. Interannual variations in mixed Rossby-gravity waves and their impacts on tropical cyclogenesis over the western North Pacific. *J. Clim.* 22(3):535–49
117. Raymond D, Bretherton C, Molinari J. 2006. Dynamics of the intertropical convergence zone of the east Pacific. *J. Atmos. Sci.* 63(2):582–97
118. Jiang X, Waliser DE. 2009. Two dominant subseasonal variability modes of the eastern Pacific ITCZ. *Geophys. Res. Lett.* 36(4):L04704
119. Jiang X, Waliser DE. 2008. Northward propagation of the subseasonal variability over the eastern Pacific warm pool. *Geophys. Res. Lett.* 35(9):L09814
120. Rydbeck AV, Maloney ED, Xie S-P, Hafner J, Shaman J. 2013. Remote forcing versus local feedback of east Pacific intraseasonal variability during boreal summer. *J. Clim.* 26(11):3575–96
121. Maloney E, Kiehl J. 2002. MJO-related SST variations over the tropical eastern Pacific during Northern Hemisphere summer. *J. Clim.* 15(6):675–89
122. Crosbie E, Serra YL. 2014. Intra-seasonal modulation of synoptic scale disturbances and tropical cyclone genesis in the eastern North Pacific. *J. Clim.* 27:5724–45. doi: 10.1175/JCLI-D-13-00399.1
123. Maloney ED, Chelton DB, Esbensen SK. 2008. Subseasonal SST variability in the tropical eastern North Pacific during boreal summer. *J. Clim.* 21(17):4149–67
124. Wen M, Yang S, Higgins W, Zhang R. 2011. Characteristics of the dominant modes of atmospheric quasi-biweekly oscillation over tropical-subtropical Americas. *J. Clim.* 24(15):3956–70
125. Molinari J, Vollaro D. 2000. Planetary- and synoptic-scale influences on eastern Pacific tropical cyclogenesis. *Mon. Weather Rev.* 128(9):3296–307
126. Aiyyer A, Molinari J. 2008. MJO and tropical cyclogenesis in the Gulf of Mexico and eastern Pacific: case study and idealized numerical modeling. *J. Atmos. Sci.* 65(8):2691–704
127. Maloney ED, Hartmann DL. 2000. Modulation of hurricane activity in the Gulf of Mexico by the Madden-Julian oscillation. *Science* 287(5460):2002–4
128. Camargo SJ, Robertson AW, Barnston AG, Ghil M. 2008. Clustering of eastern North Pacific tropical cyclone tracks: ENSO and MJO effects. *Geochem. Geophys. Geosyst.* 9(6):Q06V05
129. Zehnder JA. 1991. The interaction of planetary-scale tropical easterly waves with topography: a mechanism for the initiation of tropical cyclones. *J. Atmos. Sci.* 48(10):1217–30
130. Schultz DM, Bracken WE, Bosart LF, Hakim GJ, Bedrick MA, et al. 1997. The 1993 superstorm cold surge: frontal structure, gap flow, and tropical impact. *Mon. Weather Rev.* 125(1):5–39

131. Schultz DM, Keyser D, Bosart LF. 1998. The effect of large-scale flow on low-level frontal structure and evolution in midlatitude cyclones. *Mon. Weather Rev.* 126(7):1767–91
132. Hastenrath S. 1991. *Climate Dynamics of the Tropics: Updated Edition from Climate and Circulation of the Tropics*. Dortrecht, Neth.: Kluwer Acad.
133. Amador JA, Chacón RE, Laporte S. 2003. Climate and climate variability in the Arenal River basin of Costa Rica. In *Climate and Water*, ed. HF Diaz, BJ Morehouse, pp. 317–49. Dortrecht, Neth.: Kluwer Acad.
134. Gray WM. 1979. Hurricanes: their formation, structure and likely role in the tropical circulation. In *Meteorology Over the Tropical Oceans*, ed. DB Shaw, pp. 155–218. Bracknell, Bershire, UK: R. Meteorol. Soc.
135. Amador JA. 2008. The Intra-Americas Sea low-level jet: overview and future research. *Ann. N.Y. Acad. Sci.* 1146(1):153–88
136. Enfield D, Alfaro E. 1999. The dependence of Caribbean rainfall on the interaction of the tropical Atlantic and Pacific oceans. *J. Clim.* 12(7):2093–103
137. Magaña V, Amador J. 1999. The midsummer drought over Mexico and Central America. *J. Clim.* 12:1577–88
138. Martin ER, Schumacher C. 2011. Modulation of Caribbean precipitation by the Madden-Julian oscillation. *J. Clim.* 24(3):813–24
139. Barlow M, Salstein D. 2006. Summertime influence of the Madden-Julian Oscillation on daily rainfall over Mexico and Central America. *Geophys. Res. Lett.* 33(21):L21708
140. Amador JA. 1998. A climatic feature of the tropical Americas: the trade wind easterly jet. *Top. Meteorol. Oceanogr.* 5(2):91–102
141. Salinas JA. 2006. *Dinamica de las ondas del este y su interaccion con el flujo medio en El Caribe*. PhD Thesis. Univ. Nac. Autónoma de Mex.
142. Amador JA, Alfaro EJ, Rivera ER, Calderón B. 2010. Climatic features and their relationship with tropical cyclones over the Intra-Americas Seas. In *Hurricanes and Climate*, Vol. 2, ed. JB Eisner, RE Hodges, JC Malmstadt, KN Scheitlin, pp. 149–73. Dordrecht, Neth.: Springer
143. Janicot S, Mounier F, Hall N, Leroux SE, Sultan B, Kiladis GN. 2009. Dynamics of the west African monsoon. Part IV: Analysis of 25–90-day variability of convection and the role of the Indian monsoon. *J. Clim.* 22(6):1541–65
144. Janicot S, Mounier F, Gervois S, Sultan B, Kiladis GN. 2010. The dynamics of the west African monsoon. Part V: The detection and role of the dominant modes of convectively coupled equatorial Rossby waves. *J. Clim.* 23(14):4005–24
145. Janicot S, Thorncroft CD, Ali A, Asencio N, Berry GJ, et al. 2008. Large-scale overview of the summer monsoon over west Africa during the AMMA field experiment in 2006. *Ann. Geophys.* 26:2569–95
146. Mounier F, Janicot S, Kiladis GN. 2008. The west African monsoon dynamics. Part III: The quasi-biweekly zonal dipole. *J. Clim.* 21(9):1911–28
147. Sultan B, Janicot S, Diedhiou A. 2003. The west African monsoon dynamics. Part I: Documentation of intraseasonal variability. *J. Clim.* 16(21):3389–406
148. Mounier F, Janicot S. 2004. Evidence of two independent modes of convection at intraseasonal timescale in the west African summer monsoon. *Geophys. Res. Lett.* 31(16):L16116
149. Taylor CM. 2008. Intraseasonal land-atmosphere coupling in the west African monsoon. *J. Clim.* 21(24):6636–48
150. Cornforth RJ, Hoskins BJ, Thorncroft CD. 2009. The impact of moist processes on the African easterly jet–African easterly wave system. *Q. J. R. Meteorol. Soc.* 135(641):894–913
151. Leroux SE, Hall N, Kiladis GN. 2010. A climatological study of transient-mean-flow interactions over west Africa. *Q. J. R. Meteorol. Soc.* 136(S1):397–410
152. Hsieh J, Cook K. 2005. Generation of African easterly wave disturbances: relationship to the African easterly jet. *Mon. Weather Rev.* 133(5):1311–27
153. Hall N, Kiladis GN, Thorncroft CD. 2006. Three-dimensional structure and dynamics of African easterly waves. Part II: Dynamical modes. *J. Atmos. Sci.* 63(9):2231–45
154. Mo KC. 2000. The association between intraseasonal oscillations and tropical storms in the Atlantic basin. *Mon. Weather Rev.* 128(12):4097–107

155. Mounier F, Kiladis GN, Janicot S. 2007. Analysis of the dominant mode of convectively coupled Kelvin waves in the west African monsoon. *J. Clim.* 20(8):1487–503
156. Nguyen H, Duvel JP. 2008. Synoptic wave perturbations and convective systems over equatorial Africa. *J. Clim.* 21:6372–88
157. Guo Y, Jiang X, Waliser DE. 2014. Modulation of the convectively coupled Kelvin waves over South America and tropical Atlantic Ocean in association with the Madden-Julian oscillation. *J. Atmos. Sci.* 71:1371–88
158. Ventrice MJ, Thorncroft CD, Janiga MA. 2012. Atlantic tropical cyclogenesis: a three-way interaction between an African easterly wave, diurnally varying convection, and a convectively coupled atmospheric Kelvin wave. *Mon. Weather Rev.* 140(4):1108–24
159. Liebmann B, Kiladis GN, Carvalho L. 2009. Origin of convectively coupled Kelvin waves over South America. *J. Clim.* 22:300–15
160. Zhang C, Gottschalck J, Maloney ED. 2013. Cracking the MJO nut. *Geophys. Res. Lett.* 40:1223–30
161. Tian B, Waliser DE. 2012. Chemical and biological impacts. See Ref. 19, pp. 569–85
162. Tian B, Yung YL, Waliser DE. 2007. Intraseasonal variations of the tropical total ozone and their connection to the Madden-Julian Oscillation. *Geophys. Res. Lett.* 34:L08704
163. Li KF, Tian B, Waliser DE, Schwartz MJ, Neu JL, et al. 2012. Vertical structure of MJO-related subtropical ozone variations from MLS, TES, and SHADOZ data. *Atmos. Chem. Phys.* 12(1):425–36
164. Li KF, Tian B, Tung KK, Kuai L, Worden JR, et al. 2013. A link between tropical intraseasonal variability and Arctic stratospheric ozone. *J. Geophys. Res. Atmos.* 118:4280–89
165. Ziemke JR, Chandra S, Schoeberl MR, Froidevaux L, Read WG, et al. 2007. Intra-seasonal variability in tropospheric ozone and water vapor in the tropics. *Geophys. Res. Lett.* 34(17):L17804
166. Cooper MJ, Martin RV, Livesey NJ. 2013. Analysis of satellite remote sensing observations of low ozone events in the tropical upper troposphere and links with convection. *Geophys. Res. Lett.* 40:3761–65
167. Tian B, Waliser DE, Kahn RA, Li Q, Yung YL, et al. 2008. Does the Madden-Julian Oscillation influence aerosol variability? *J. Geophys. Res. Atmos.* 113:D12215
168. Tian B, Waliser DE, Kahn RA, Wong S. 2011. Modulation of Atlantic aerosols by the Madden-Julian Oscillation. *J. Geophys. Res. Atmos.* 116:D15108
169. Guo Y, Tian B, Kahn RA, Kalashnikova O, Wong S, Waliser DE. 2013. Tropical Atlantic dust and smoke aerosol variations related to the Madden-Julian Oscillation in MODIS and MISR observations. *J. Geophys. Res. Atmos.* 118:4947–63
170. Zuluaga MD, Webster PJ, Hoyos CD. 2012. Variability of aerosols in the tropical Atlantic Ocean relative to African easterly waves and their relationship with atmospheric and oceanic environments. *J. Geophys. Res. Atmos.* 117:D16207
171. Reid JS, Xian P, Hyer EJ, Flatau MK, Ramirez EM, et al. 2012. Multi-scale meteorological conceptual analysis of observed active fire hotspot activity and smoke optical depth in the Maritime Continent. *Atmos. Chem. Phys.* 12(4):2117–47
172. DeWitt HL, Coffman DJ, Schulz KJ, Brewer WA, Bates T, Quinn PK. 2013. Atmospheric aerosol properties over the equatorial Indian Ocean and the impact of the Madden-Julian Oscillation. *J. Geophys. Res. Atmos.* 118:5736–49
173. Ragsdale KM, Barrett BS, Testino AP. 2013. Variability of particulate matter (PM_{10}) in Santiago, Chile by phase of the Madden-Julian Oscillation (MJO). *Atmos. Environ.* 81:304–10
174. Li KF, Tian B, Waliser DE, Yung YL. 2010. Tropical mid-tropospheric CO_2 variability driven by the Madden-Julian oscillation. *Proc. Natl. Acad. Sci. USA* 107(45):19171–75
175. Lin J-L, Kiladis GN, Mapes BE, Weickmann KM, Sperber KR, et al. 2006. Tropical intraseasonal variability in 14 IPCC AR4 climate models. Part I: Convective signals. *J. Clim.* 19(12):2665–90
176. Tulich SN, Kiladis GN, Suzuki-Parker A. 2011. Convectively coupled Kelvin and easterly waves in a regional climate simulation of the tropics. *Clim. Dyn.* 36(1–2):185–203
177. Wang Y, Xie SP, Xu H, Wang B. 2004. Regional model simulations of marine boundary layer clouds over the southeast Pacific off South America. Part I: Control experiment. *Mon. Weather Rev.* 132:274–96
178. Wang Y, Xu H, Xie SP. 2004. Regional model simulations of marine boundary layer clouds over the southeast Pacific off South America. Part II: Sensitivity experiments. *Mon. Weather Rev.* 132:2650–68

179. Small RJ, Xie S-P, Maloney ED, de Szoeke SP, Miyama T. 2011. Intraseasonal variability in the Far-East Pacific: investigation of the role of air-sea coupling in a regional coupled model. *Clim. Dyn.* 36(5–6):867–90
180. Hagos S, Leung LR, Dudhia J. 2011. Thermodynamics of the Madden-Julian oscillation in a regional model with constrained moisture. *J. Atmos. Sci.* 68(9):1974–89
181. Lin J-L, Lee M-I, Kim D, Kang I-S, Frierson DMW. 2008. The impacts of convective parameterization and moisture triggering on AGCM-simulated convectively coupled equatorial waves. *J. Clim.* 21(5):883–909
182. Frierson DM, Kim D, Kang I-S, Lee M-I, Lin J. 2011. Structure of AGCM-simulated convectively coupled Kelvin waves and sensitivity to convective parameterization. *J. Atmos. Sci.* 68(1):26–45
183. Zhou L, Neale RB, Jochum M, Murtugudde R. 2012. Improved Madden-Julian oscillations with improved physics: the impact of modified convection parameterizations. *J. Clim.* 25(4):1116–36
184. Holloway CE, Woolnough SJ, Lister GMS. 2013. The effects of explicit versus parameterized convection on the MJO in a large-domain high-resolution tropical case study. Part I: Characterization of large-scale organization and propagation. *J. Atmos. Sci.* 70(5):1342–69
185. Thayer-Calder K, Randall DA. 2009. The role of convective moistening in the Madden-Julian oscillation. *J. Atmos. Sci.* 66(11):3297–312
186. Hannah WM, Maloney ED. 2011. The role of moisture-convection feedbacks in simulating the Madden-Julian oscillation. *J. Clim.* 24(11):2754–70
187. Benedict JJ, Maloney ED, Sobel AH, Frierson DM, Donner LJ. 2013. Tropical intraseasonal variability in version 3 of the GFDL atmosphere model. *J. Clim.* 26(2):426–49
188. Kim D, Xavier P, Maloney E, Wheeler M, Waliser D, et al. 2014. Process-oriented MJO simulation diagnostic: moisture sensitivity of simulated convection. *J. Clim.* 27:5379–95
189. Maloney ED, Sobel AH, Hannah WM. 2010. Intraseasonal variability in an aquaplanet general circulation model. *J. Adv. Model. Earth Syst.* 2:1–24
190. Andersen JA, Kuang Z. 2012. Moist static energy budget of MJO-like disturbances in the atmosphere of a zonally symmetric aquaplanet. *J. Clim.* 25:2782–804
191. Pritchard MS, Bretherton CS. 2013. Causal evidence that rotational moisture advection is critical to the superparameterized Madden-Julian oscillation. *J. Atmos. Sci.* 71:800–815
192. Maloney ED. 2009. The moist static energy budget of a composite tropical intraseasonal oscillation in a climate model. *J. Clim.* 22(3):711–29
193. Miyakawa T, Takayabu YN, Nasuno T, Miura H, Satoh M, Moncrieff MW. 2012. Convective momentum transport by rainbands within a Madden-Julian oscillation in a global nonhydrostatic model with explicit deep convective processes. Part I: Methodology and general results. *J. Atmos. Sci.* 69(4):1317–38
194. Straub KH, Haertel PT, Kiladis GN. 2010. An analysis of convectively coupled Kelvin waves in 20 WCRP CMIP3 global coupled climate models. *J. Clim.* 23(11):3031–56
195. Mapes BE. 2000. Convective inhibition, subgrid-scale triggering energy, and stratiform instability in a toy tropical wave model. *J. Atmos. Sci.* 57(10):1515–35
196. Kuang Z. 2008. A moisture-stratiform instability for convectively coupled waves. *J. Atmos. Sci.* 65:834–54
197. Jiang X, Waliser DE, Kim D, Zhao M, Sperber KR, et al. 2012. Simulation of the intraseasonal variability over the eastern Pacific ITCZ in climate models. *Clim. Dyn.* 39(3–4):617–36
198. Jiang X, Maloney ED, Li J-LF, Waliser DE. 2013. Simulations of the eastern North Pacific intraseasonal variability in CMIP5 GCMs. *J. Clim.* 26(11):3489–510
199. Sheffield J, Langenbrunner B, Meyerson JE, Neelin JD, Camargo SJ, et al. 2013. North American climate in CMIP5 experiments. Part II: Evaluation of historical simulations of intra-seasonal to decadal variability. *J. Clim.* 26:9247–90
200. Kozar ME, Misra V. 2012. Evaluation of twentieth-century Atlantic warm pool simulations in historical CMIP5 runs. *Clim. Dyn.* 41(9–10):2375–91
201. Waliser D. 2012. Predictability and forecasting. See Ref. 19, pp. 433–76
202. Vitart F, Woolnough S, Balmaseda MA, Tompkins AM. 2007. Monthly forecast of the Madden-Julian oscillation using a coupled GCM. *Mon. Weather Rev.* 135(7):2700–715

203. Agudelo PA, Hoyos CD, Webster PJ, Curry JA. 2008. Application of a serial extended forecast experiment using the ECMWF model to interpret the predictive skill of tropical intraseasonal variability. *Clim. Dyn.* 32(6):855–72
204. Vitart F, Leroy A, Wheeler MC. 2010. A comparison of dynamical and statistical predictions of weekly tropical cyclone activity in the Southern Hemisphere. *Mon. Weather Rev.* 138:3671–82
205. Seo K-H, Wang W, Gottschalck J, Zhang Q, Schemm J-KE, et al. 2009. Evaluation of MJO forecast skill from several statistical and dynamical forecast models. *J. Clim.* 22(9):2372–88
206. Zhang Q, van den Dool H. 2012. Relative merit of model improvement versus availability of retrospective forecasts: the case of Climate Forecast System MJO prediction. *Weather Forecast.* 27:1045–51
207. Wang W, Hung M-P, Weaver SJ, Kumar A, Fu X. 2013. MJO prediction in the NCEP Climate Forecast System version 2. *Clim. Dyn.* 42:2509–20
208. Rashid HA, Hendon HH, Wheeler MC, Alves O. 2010. Prediction of the Madden-Julian oscillation with the POAMA dynamical prediction system. *Clim. Dyn.* 36(3–4):649–61
209. Neena JM, Lee JY, Waliser DE, Wang B, Jiang X. 2014. Predictability of the Madden-Julian Oscillation (MJO) in the Intraseasonal Variability Hindcast Experiment (ISVHE). *J. Clim.* 27:4531–43. doi: 10.1175/JCLI-D-13-00624.1
210. Bechtold P, Köhler M, Jung T. 2008. Advances in simulating atmospheric variability with the ECMWF model: from synoptic to decadal time-scales. *Q. J. R. Meteorol. Soc.* 134:1337–51
211. Hirons LC, Inness P, Vitart F, Bechtold P. 2012. Understanding advances in the simulation of intraseasonal variability in the ECMWF model. Part I: The representation of the MJO. *Q. J. R. Meteorol. Soc.* 139:1417–26
212. Hirons LC, Inness P, Vitart F, Bechtold P. 2012. Understanding advances in the simulation of intraseasonal variability in the ECMWF model. Part II: The application of process-based diagnostics. *Q. J. R. Meteorol. Soc.* 139:1427–44
213. Hannah WM, Maloney ED. 2014. The moist static energy budget in NCAR CAM5 hindcasts during DYNAMO. *J. Adv. Model. Earth Syst.* 6(2):420–40. doi: 10.1002/2013MS000272
214. Jiang X, Waliser DE, Wheeler MC, Jones C, Lee M-I, Schubert SD. 2008. Assessing the skill of an all-season statistical forecast model for the Madden-Julian oscillation. *Mon. Weather Rev.* 136(6):1940–56
215. Elsberry RL, Jordan MS, Vitart F. 2010. Predictability of tropical cyclone events on intraseasonal timescales with the ECMWF monthly forecast model. *Asia Pac. J. Atmos. Sci.* 46(2):135–53
216. Belanger JI, Curry JA, Webster PJ. 2010. Predictability of North Atlantic tropical cyclone activity on intraseasonal time scales. *Mon. Weather Rev.* 138:4362–74
217. Gall JS, Ginis I, Lin S-J, Marchok TP, Chen J-H. 2011. Experimental tropical cyclone prediction using the GFDL 25-km-resolution global atmospheric model. *Weather Forecast.* 26(6):1008–19
218. Winker DM, Pelon J. 2003. The CALIPSO mission. *Proc. IEEE* 2:1329–31
219. Meehl GA, Moss RH, Taylor KE, Eyring V, Stouffer RJ, et al. 2014. Climate model intercomparisons: preparing for the next phase. *Eos Trans. Am. Geophys. Union* 95(9):77–78

Annual Review of Environment and Resources

Volume 39, 2014

Contents

IV. Management and Governance of Resources and Environment

V. Methods and Indicators

Indexes

Errata

An online log of corrections to *Annual Review of Environment and Resources* articles may be found at http://www.annualreviews.org/errata/environ